2

CORRECTIONS TO PHOTO COORDINATES

Surveying Engineering Department
Ferris State University

Analytical Photogrammetry Instrumentation

Analytical photogrammetry is performed on specialized instruments that have a very high cost due to the fact that there is a limited market. With the onset of digital photogrammetry, the instrumentation is cheaper (being the computer) but the software still remains expensive for this specialized applications.

The design characteristics of analytical instrumentation include [Merchant, 1979]:

- High accuracy
- High reliability
- High measuring efficiency
- Low first cost
- Low cost of maintenance

In addition, operational efficiency becomes an important consideration. This factor involves the necessary training required for the operator of the equipment. If the instrument requires an individual with a basic theoretical background in photogrammetry along with experience, then there will be a limited pool from which one can draw their operators. Operational efficiency also involves on the comfort of the operator when operating the equipment. One of the advantages of digital photogrammetry is that it has the capability, at least theoretically, to completely automate the whole process and an individual with no basic understanding of photogrammetric principles can do this.

There are various different kinds of photogrammetric instrumentation that can be used in analytical photogrammetry. At the low end, precision analog, or semi-analytical (computer-aided) stereoplotters can be used either in a monoscopic or stereoscopic mode. When used on a stereoplotter, it is important to put all of the elements in their zero positions ($\omega' = \omega'' = \varphi' = \varphi'' = \kappa' = \kappa'' = by' = by'' = bz' = bz'' = 0$) [Ghosh, 1979]. The base (bx), scale and Z-column readings should be at some realistic value. Analytical plotters can also be used for analytical photogrammetric measurements. These instruments are generally linked to analytical photogrammetry software that helps the operator complete the photo measurements.

Comparators are designed specifically for precise photo measurements for analytical photogrammetry. Comparators can be either monoscopic or stereoscopic. The photographs are placed on the stages and all points that are imaged on the photo are measured. The last type of instrument is the digital or softcopy plotter. Photos are scanned (or captured directly in a digital form) and points are measured. With autocorrelation techniques the whole process of aerotriangulation can be automated with the solution containing more points than can be done manually.

To achieve the high accuracy demanded by many analytical photogrammetric applications, it is important that the instrument upon which the measurements are made is well calibrated and maintained. There are many systematic error sources associated with the comparator. They are

> “a) Errors of the instrument system,
> - scaling and periodic errors (of the x, y measuring systems involving scales, spindles, coordinate counter, etc.);
> - affinity errors (being the scale difference between x an y directions);
> - errors of rectilinearity (bending) of the guide rails;
> - lack of orthogonality between x and y axes (also known as ‘rectangularity error’).
>
> b) Backlash and tracking errors.
>
> c) Dynamic errors (e.g., microscope velocity does not drop to zero at points to be approached during the operation.
>
> d) Errors of automation in the system,
> - digital resolution (smallest incremental interval);
> - errors due to deviation of the direction. This is because the control system may not provide for the continuously variable scanning direction.”
>
> [Ghosh, 1979, p.30]

One could determine the corrections to each of these error sources, although from a practical perspective these errors are accounted for by transforming the photo measurements to the “true” photo system, which is based on calibration.

Ground Targets

Ground targets can be one of three different types. Signalized points are targeted on the ground prior to the flight. Several different target designs are used in photogrammetry. Detail points are those well defined physical features that are imaged on the photography. These items can be things like the intersection of roads (for small-scale mapping), intersections of sidewalks, manholes, etc. The last type of control point is the artificial point that is added to the photography after the film is processed. Using a point transfer instrument, such as the PUG by Wild, points are marked on the emulsion of the film.

Example target design employed by the Michigan Department of Transportation are shown in figures 1-3.

Standard Aerial Photography Targets

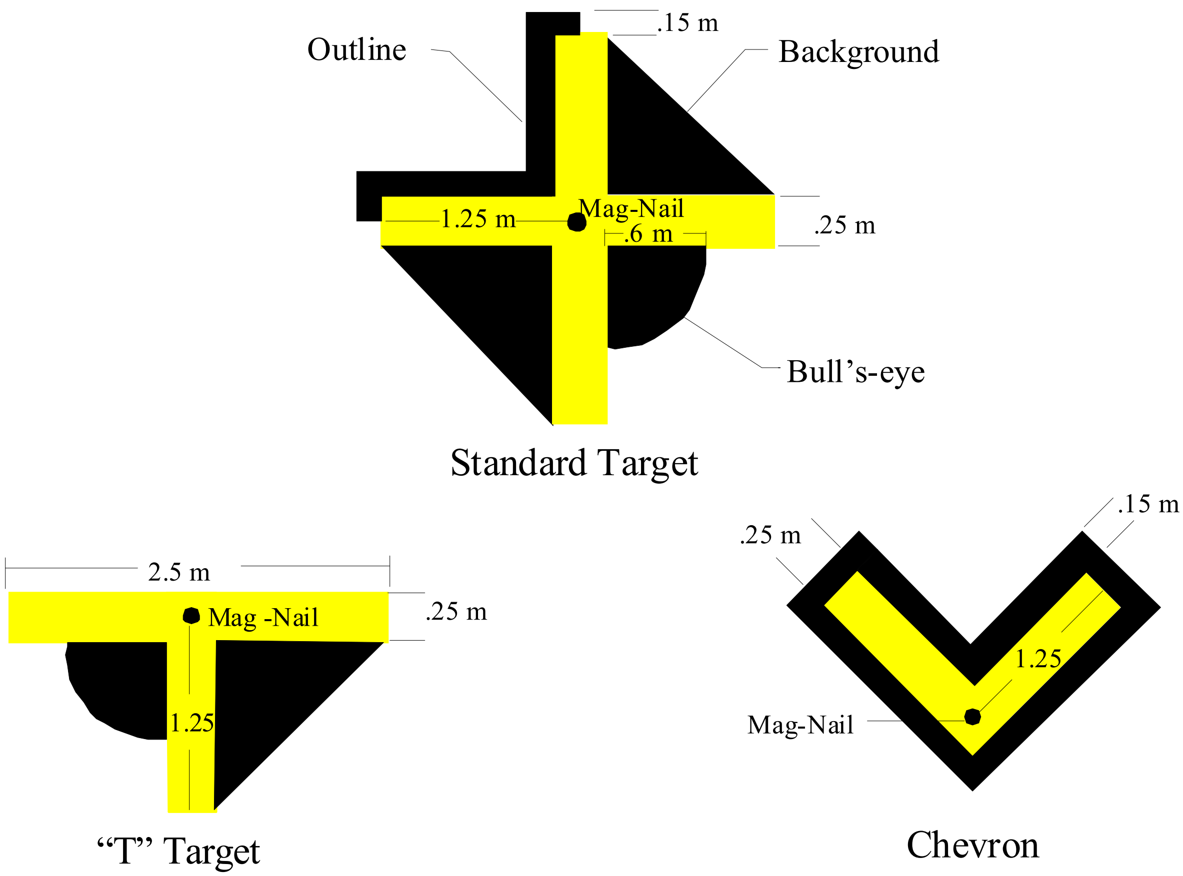

All painted targets must be highlighted in black by one of the following methods:

a. Background
b. Outline
c. Bull's-eye

Figure 1. Standard MDOT target design.

High Level Aerial Photography Targets

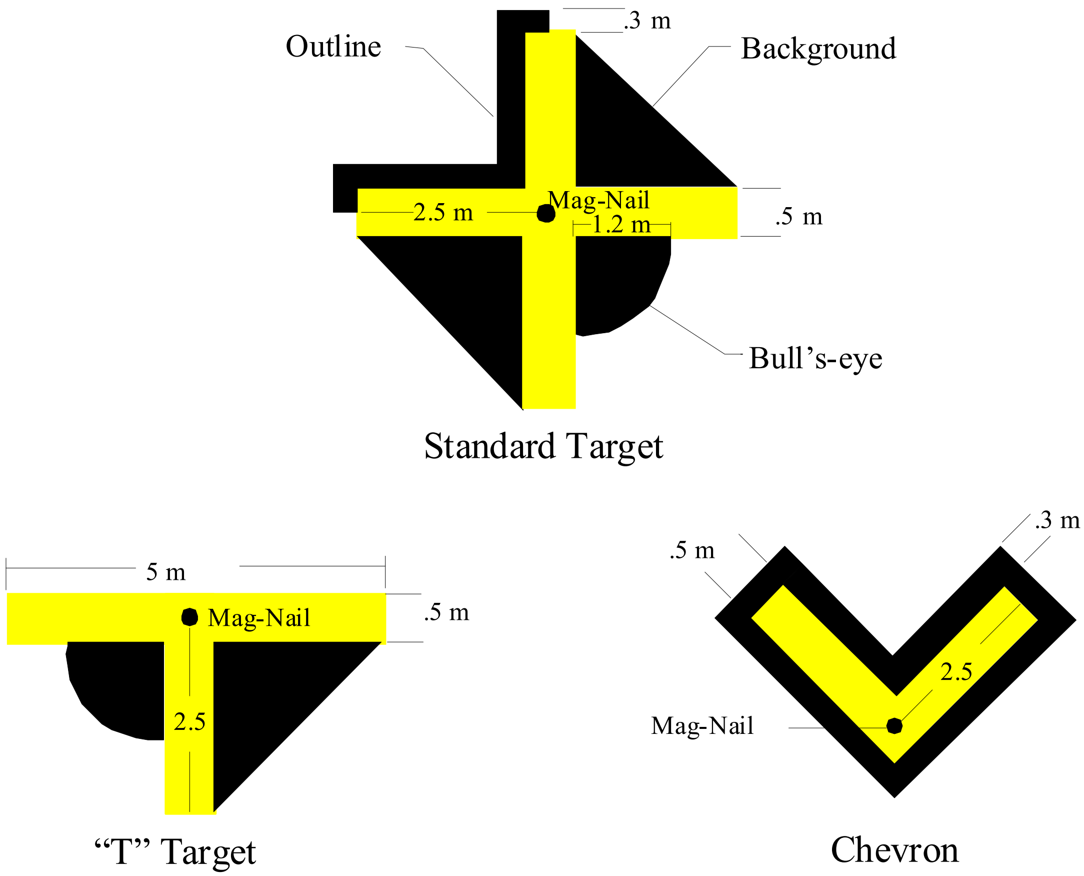

All painted targets must be highlighted in black by one of the following methods:

1. Background
2. Outline
3. Bull's-eye

Figure 2. MDOT target design for high altitude photography.

Low Level Aerial Photography Targets

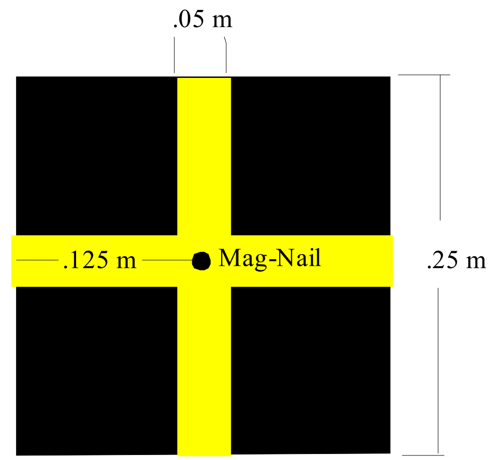

Low Level Target

Low Level target must have the square black outline shown.

Figure 3. Low level MDOT target design.

Abbe's Comparator Principle

Abbe's comparator principle states that the object that is to be measured and the measuring instrument must be in contact or lie in the same plane. The design is based on the following requirements (refer to figure 4):

"i) To exclusively base the measurement in all cases on a longitudinal graduation with which the distance to be measured is directly compared; and

ii) To always design the measuring apparatus in such a way that the distance to be measured will be the rectilinear extension of the graduation used as a scale." [Manual of Photogrammetry, ASP, in Ghosh, 1979, p.7]

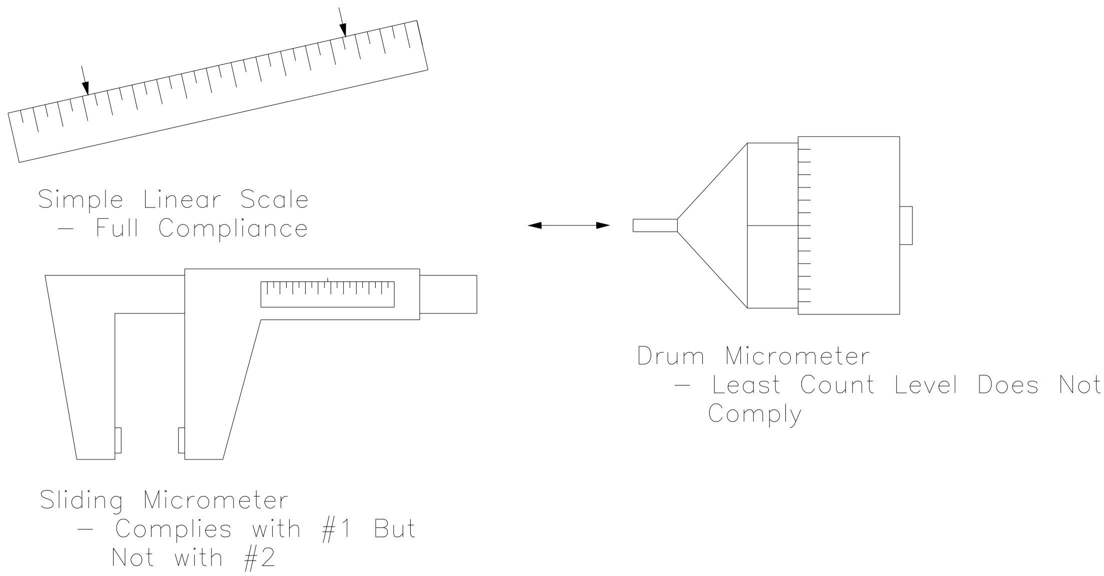

Figure 4. Example of Abbe's comparator principle with simple measurement systems.

Photo measurements can be made on many different types of instruments. In the past, the most accurate methods involved the use of a comparator and different types of comparators were created to improve the accuracy of these measurements. Today, digital photogrammetric techniques can be employed for photo measurements with a very high degree of accuracy.

While comparators come in all different types of configurations, the procedure described as follows will illustrate an approach to determining photo coordinates from comparator measurements. This approach is the same that can be applied to the Mann monocomparator. The geometry is depicted in figure 5. The simplest method, computationally, is to place the diapositive on the rotary stage and align the fiducial marks to the coordinate system of the comparator. This is done by rotating the stage such that the line between the fiducial marks labeled 1 and 2 lie are perfectly aligned to the comparator x-axis. Then, the comparator coordinates to the indicated principal point can be found using:

$$r_{x_o} = \frac{r_{x_3} + r_{x_4}}{2}$$

$$r_{y_o} = r_{y_1} = r_{y_2}$$

The corresponding photo coordinates are found by subtracting the comparator coordinates of the indicated principal point to the corresponding comparator measurements made at each point. For point p, this is

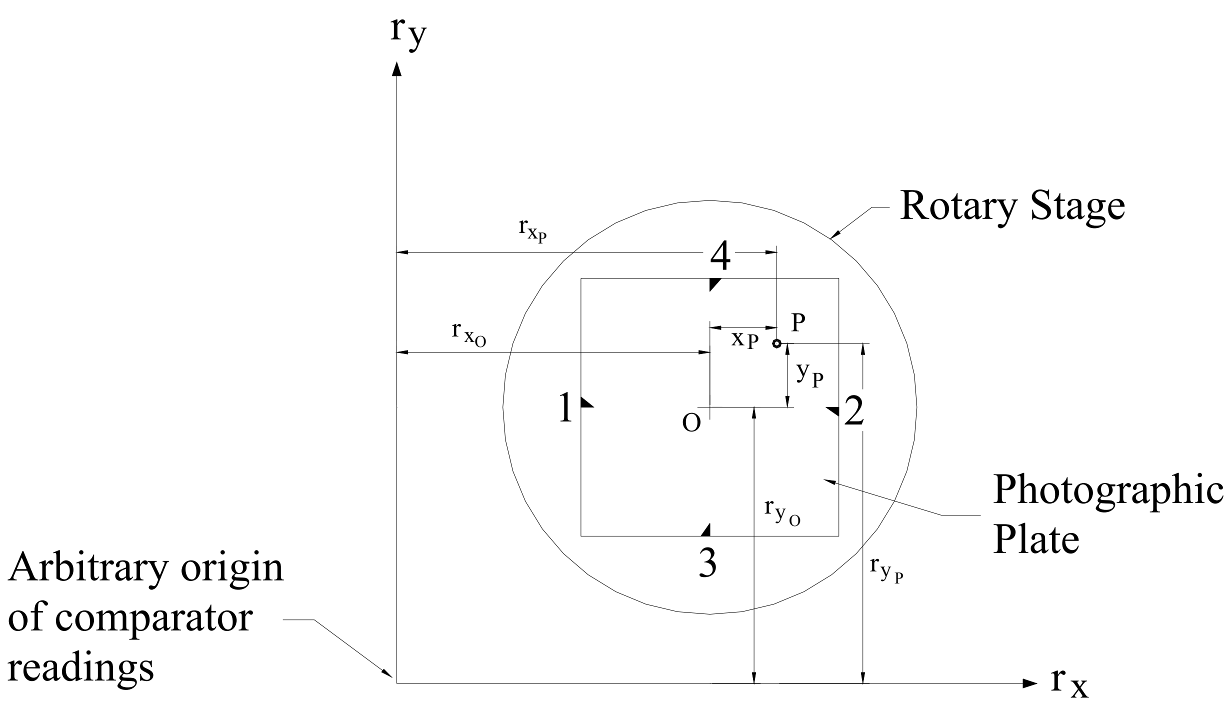

Figure 5. Geometry of a rotary stage comparator.

$$x_p = r_{x_p} - r_{x_o}$$

$$y_p = r_{y_p} - r_{y_o}$$

The process of aligning the fiducial marks to the comparator x-axis is a laborious procedure that is not necessary. Simply place the diapositive onto the comparator rotary stage such that it is approximately aligned to the comparator coordinate system. Then, observe the coordinates at each of the fiducial coordinates and perform a transformation from the comparator coordinate system to the photo coordinate system. The rotation angle can be found using the arctangent function

$$\tan\theta = \frac{r_{y_2} - r_{y_1}}{r_{x_2} - r_{x_1}}$$

Then, apply a 2-dimensional transformation.

$$x' = r_x \cos\theta + r_y \sin\theta$$
$$y' = -r_x \sin\theta + r_y \cos\theta$$

Using this basic relationship, the y' coordinates of fiducial points 1 or 2 and the x' coordinates of fiducial points 3 and 4 need only be computed. Then,

$$x'_o = \frac{x'_3 + x'_4}{2}$$

$$y'_o = y'_1 = y'_2$$

and

$$x_p = x'_p - x'_o$$

$$y_p = y'_p - y'_p$$

If, as is the normal situation, the coordinates of the fiducial points on the camera calibration report are in the photo coordinate system then there is no need to determine the transformed coordinates of the indicated principal point and perform the translation to the origin. The transformed coordinates will represent the photo coordinates directly.

Basic Analytical Photogrammetric Theory

Analytical photogrammetry can be broken down into three fundamental categories: First Order Theory, Second Order Theory and Third Order Theory. **Fist Order Theory** is the basic collinearity concept where the light rays from the object space pass through the atmosphere and the camera lens to the film in a straight line. **Second Order Theory** corrects for the most significant errors that are not accounted for in First Order Theory. Those items that are normally covered include lens distortion, atmospheric refraction, film deformation and earth curvature. **Third Order Theory** consists of all the other sources of error in the imposition of the collinearity condition, which are not included in Second Order Theory. These errors are usually not accounted for except for special circumstances. They include platen unflatness, transient thermal gradients across the lens cone, etc.

Interior Orientation

The first phase of analytical photogrammetric processing is the determination of the interior orientation of the photography. The photogrammetric coordinate system is shown in figure 6. The point, p, is imaged on the photograph with coordinates x_p, yp, 0. The principal point is determined through camera calibration and it generally is reported with respect to the center of the photograph as defined by the intersection of opposite fiducial marks (indicated principal point). It has coordinates x_o, y_o, 0. The perspective center is the location of the lens elements and it has coordinates x_o, y_o, f. The vector from the perspective center to the position on the photo is given as

$$\vec{a} = \begin{bmatrix} x_p - x_o \\ y_p - y_o \\ 0 - f \end{bmatrix}$$

Interior orientation involves the determination of film deformation, lens distortion, atmospheric refraction, and earth curvature. The purpose is to correct the image rays such that the line form the object space to the image space is a straight line, thereby fulfilling the basic assumption used in the collinearity condition.

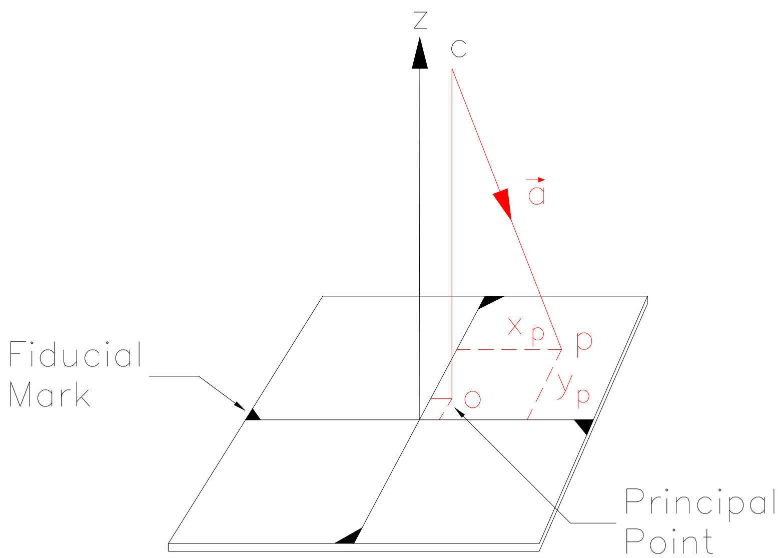

Figure 6. Photographic coordinate system.

Film Deformation

When film is processed and used it is susceptible to dimensional change due to the tension applied to the film as it is wound during both the picture taking and processing stages. In addition, the introduction of water-based chemicals to the emulsion during processing and the subsequent drying of the film may cause the emulsion to change dimensionally. Therefore, these effects need to be compensated. The simplest approach is to use the appropriate transformation model discussed in the previous section.

One of the problems with this approach is that it is possible that unmodelled distortion can still be present when only four (or fewer) fiducial marks are employed. To overcome this problem, reseau photography is commonly employed for applications requiring a higher degree of accuracy. A reseau grid consists of a grid of targets that are fixed to the camera lens and imaged on the film. One simple approach is to put a piece of glass in front of the film with the targets etched on the surface. The reseau grid is calibrated so that the positions of the targets are accurately known. By observing the reseau targets that surround the imaged points and using one of the transformation models discussed earlier, the results should more accurately depict the dimensional changes that occur due to film deformation. For example, the isogonal affine model can be used. It will have the following form, taking into consideration the coordinates of the principal point (x_o, y_o).

$$\begin{bmatrix} x \\ y \end{bmatrix} = \begin{bmatrix} \Delta x \\ \Delta y \end{bmatrix} + \begin{bmatrix} \cos\alpha & \sin\alpha \\ -\sin\alpha & \cos\alpha \end{bmatrix} \begin{bmatrix} x' \\ y' \end{bmatrix} - \begin{bmatrix} x_o \\ y_o \end{bmatrix}$$

In its linear form it looks like:

$$\begin{bmatrix} x \\ y \end{bmatrix} = \begin{bmatrix} a & b \\ -b & a \end{bmatrix} \begin{bmatrix} x' \\ y' \end{bmatrix} + \begin{bmatrix} c \\ d \end{bmatrix} - \begin{bmatrix} x_o \\ y_o \end{bmatrix}$$

Using 4 fiducials, an 8-parameter projective transformation can be used. Its advantage is that linear scale changes can be found in any direction. The correction for film deformation is given as

$$x = \frac{a_1 x' + a_2 y' + a_3}{c_1 x' + c_2 y' + 1} - x_o$$

$$y = \frac{b_1 x' + b_2 y' + b_3}{c_1 x' + c_2 y' + 1} - y_o$$

Measurement of the four fiducials yields 8 observations. Therefore, this model provides a unique solution.

Other approach to compensation of film deformation is to use a polynomial. One model, used by the U.S. Coast and Geodetic Survey (now National Geodetic Survey) when four fiducials are used is shown as:

$$\Delta x = x - x' = x + a_0 + a_1 x + a_2 y + a_3 xy$$
$$\Delta y = y - y' = y + b_0 + b_1 x + b_2 y + b_3 xy$$

This model can be expanded to an eight fiducial observational scheme as:

$$\Delta x = x - x' = x + a_0 + a_1 x + a_2 y + a_3 xy + a_4 x^2 + a_5 y^2 + a_6 x^2 y + a_7 xy$$
$$\Delta y = y - y' = y + b_0 + b_1 x + b_2 y + b_3 xy + b_4 x^2 + b_5 y^2 + b_6 x^2 y + b_7 xy$$

Lens Distortion

The effects of lens distortion are to move the image from its theoretically correct location to its actual position. There are two components of lens distortion: radial distortion (Seidel aberration) and decentering distortion. Radial lens distortion is caused from faulty grinding of the lens. With today's computer controlled lens manufacturing process, this distortion is almost negligible at least to the accuracy of the camera calibration itself. Decentering distortion is caused by faulty placement of the individual lens elements in the camera cone and other manufacturing defects. The effects are small with today's lens systems. The values for lens distortion are determined from camera calibration. These values are generally reported by either a table or in terms of a polynomial (see the example at the end of this section).

Seidel Aberration Distortion

Seidel has identified five lens aberrations. These include astigmatism, chromatic aberration (this is sometimes broken into lateral and longitudinal chromatic aberration), spherical aberration, coma, curvature of field, and distortion. An aberration is the "failure of an optical system to bring all light rays received from a point object to a single image point or to a prescribed geometric position" [ASPRS, 1980]. It is caused by the faulty grinding of the lens. Generally, aberrations do not affect the geometry of the image but instead affect image quality. The exception is Seidel's fifth aberration - distortion. Here the geometric position of the image point is moved in image space and this change in position must be accounted for in analytical photogrammetry. The effect of this distortion is radial from the principal point.

Conrady's intuitive development for handling this radial distortion is expressed in the following polynomial form:

$$\delta r = k_0 r + k_1 r^3 + k_2 r^5 + k_3 r^7 + k_4 r^9 + \cdots$$

This is based on three general hypotheses:

"a. The axial ray passes the lens undeviated;

b. The distortion can be represented by a continuous function; and

c. The sense of the distortions should be positive for all outward displacement of the image." [Ghosh, 1979, p.88]

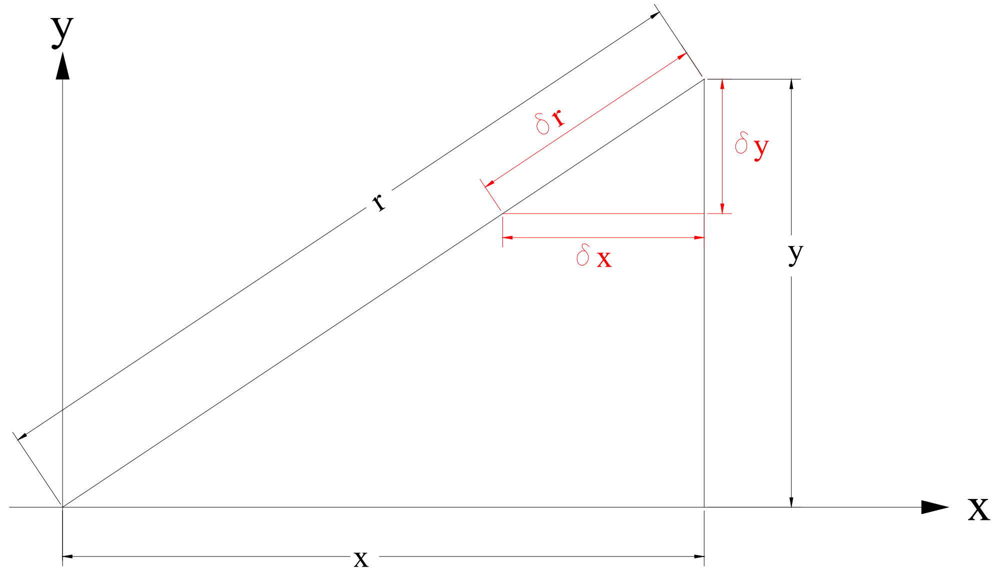

Figure 7. Radial lens distortion geometry.

From Figure 7, recall that

$$r^2 = x^2 + y^2$$

By similar triangles, the following relationship can be shown

$$\frac{\delta r}{r} = \frac{\delta x}{x} = \frac{\delta y}{y}$$

the x and y Cartesian coordinate components of the effects of this distortion are thus found by:

$$\delta x = \frac{\delta r}{r} x = \left(k_0 + k_1 r^2 + k_2 r^4 + \cdots\right) x$$

$$\delta y = \frac{\delta r}{r} y = \left(k_0 + k_1 r^2 + k_2 r^4 + \cdots\right) y$$

The corrected photo coordinates can then be computed using the form[1]:

$$x_c = x - \delta x = \left(1 - \frac{\delta r}{r}\right)x = \left(1 - k_0 - k_1 r^2 - k_2 r^4 - \cdots\right)x$$

$$y_c = y - \delta y = \left(1 - \frac{\delta r}{r}\right)y = \left(1 - k_0 - k_1 r^2 - k_2 r^4 - \cdots\right)y$$

An example using two different methods of applying the lens distortion are as follows. The first example uses a linear interpolation using the values given in the table on radial lens distortion from a camera calibration report. The second example is the same as the first except that this time the polynomial correction is employed. The problem is stated as follows:

A camera calibration report displays the following information:

Field Angle	7.5^0	15^0	22.7^0	30^0	35^0	40^0
Symmetric radial distortion, μm	4	6	4	-1	-6	-3
Decentering distortion, μm	0	0	0	1	1	2

If the photo coordinates of a point are x = +33.148 mm and y = -14.921 mm, what are the coordinates corrected for radial lens distortion? The calibrated focal length of the camera is 152.560 mm.

[1] Note that the U.S. Geological Survey gives the polynomial coefficients as correction terms instead of error terms as presented here. Therefore, the corrected photo coordinates are computed from the data given in the calibration report as follows:

$$x_c = \left(1 + k_0 + k_1 r^2 + k_2 r^4 + \cdots\right)x$$
$$y_c = \left(1 + k_0 + k_1 r^2 + k_2 r^4 + \cdots\right)y$$

Correcting Photographic Coordinates for Radial Lens Distortion

Given the following values:

$x := 33.148$ $y := -14.921$ $f := 152.560$

Factor to convert degrees into radians: $torad := \frac{\pi}{180}$

$$ang := \begin{pmatrix} 7.5 \\ 15 \\ 22.7 \\ 30 \\ 35 \\ 40 \end{pmatrix} \qquad distort := \begin{pmatrix} 4 \\ 6 \\ 5 \\ -1 \\ -6 \\ -3 \end{pmatrix}$$

To compute the distortion at the point, we first need to compute the radial distance from the principal point

$$dist := f \cdot \tan(ang \cdot torad) \qquad dist = \begin{pmatrix} 20.085 \\ 40.878 \\ 63.817 \\ 88.081 \\ 106.824 \\ 128.013 \end{pmatrix}$$

The radial distance from the principal point to the point is:

$$r := \sqrt{x^2 + y^2} \qquad r = 36.351$$

Thus, the point lies between the 7.5 and 15⁰ field angles. Perform a linear interpolation to find the radial distortion at that point.

$$\delta r := \frac{\left[4 + \left(\frac{distort_1 - distort_0}{dist_1 - dist_0}\right) \cdot \left(dist_1 - r\right)\right]}{1000} \qquad \delta r = 0.0044$$

The corrected photographic coordinates become:

$$x_c := \left(1 - \frac{\delta r}{r}\right) \cdot x \qquad x_c = 33.144$$

$$y_c := \left(1 - \frac{\delta r}{r}\right) \cdot y \qquad y_c = -14.919$$

Correcting Photographic Coordinates for Radial Lens Distortion

Given the following values:

$x := 33.148$ $y := -14.921$ $f := 152.560$ $r := \sqrt{x^2 + y^2}$

$k_0 := -0.2231 \times 10^{-3}$ $k_1 := 0.4501 \cdot 10^{-7}$ $k_2 := -0.1817 \cdot 10^{-11}$

Using the polynomial to compute the photographic coordinates corrected for radial lens distortion:

$$x_c := \left(1 + k_0 + k_1 \cdot r^2 + k_2 \cdot r^4\right) \cdot x \qquad x_c = 33.142$$

$$y_c := \left(1 + k_0 + k_1 \cdot r^2 + k_2 \cdot r^4\right) \cdot y \qquad y_c = -14.919$$

DECENTERING DISTORTION

Decentering lens distortion is asymmetric about the principal point of autocollimation. When the value is "one" then the radial line remains straight. This is called the axis of zero tangential distortion (see figures 8 and 9).

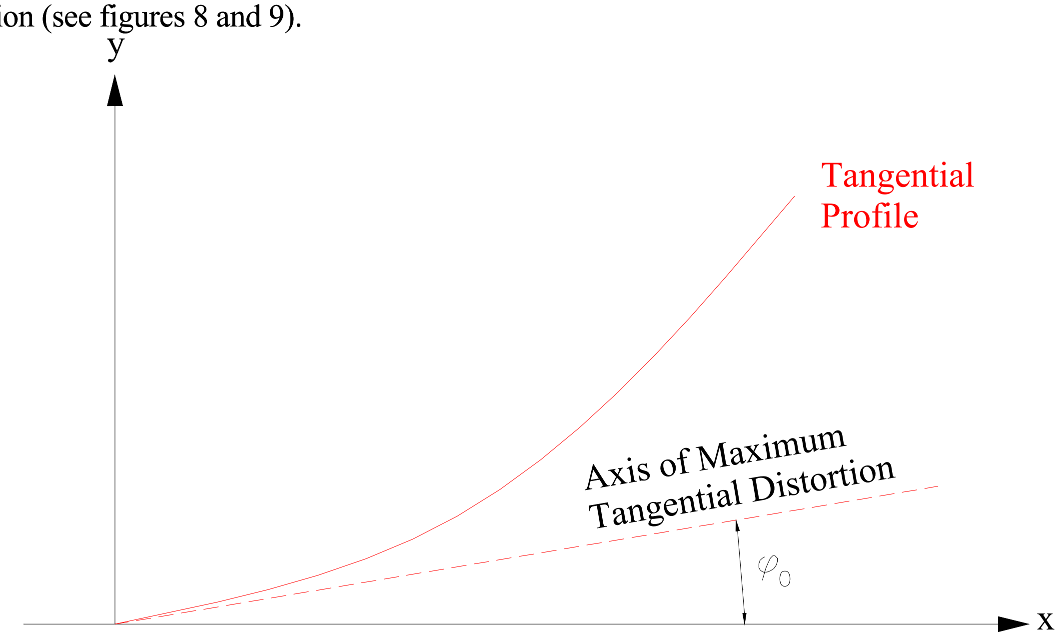

Figure 8. Geometry of tangential distortion showing the tangential profile.

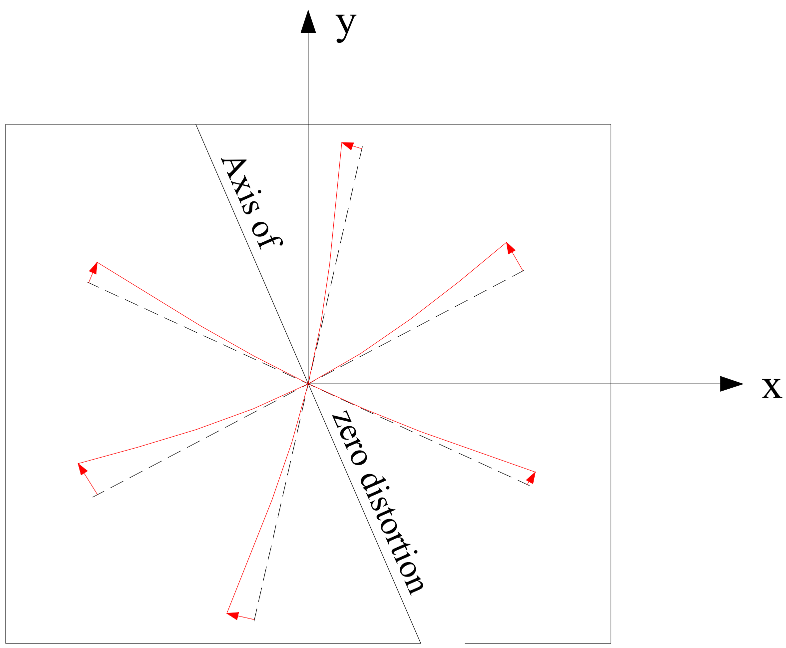

Figure 9. Effects of decentering distortion.

Duane Brown, using the developments by Washer, designed the corrections for the lens distortion due to decentering. Brown called this the "Thin Prism Model" and it is shown as:

$$\delta x = -\left(J_1 r^2 + J_2 r^4\right)\sin\varphi_o = -J\sin\varphi_o$$
$$\delta y = \left(J_1 r^2 + J_2 r^4\right)\cos\varphi_o = J\cos\varphi_o$$

where: J_1, J_2 are the coefficients of the profile function of the decentering distortion, and φ_o is the angle subtended by the axis of the maximum tangential distortion with the photo x-axis.

The concept of the thin prism was found to be inadequate to fully describe the effects of decentering distortion. Therefore, the Conrady-Brown model was developed to find the effects of decentering on the x,y encoders:

$$\delta x = \left(J_1 r^2 + J_2 r^4\right)\left[\left(1 - \frac{2x^2}{r^2}\right)\sin\varphi_o - \frac{2xy}{r^2}\cos\varphi_o\right]$$

$$\delta y = \left(J_1 r^2 + J_2 r^4\right)\left[\frac{2xy}{r^2}\sin\varphi_o - \left(1 + \frac{2y^2}{r^2}\right)\cos\varphi_o\right]$$

A revised Conrady-Brown model made further refinements to the computation of decentering distortion and this model is shown to be:

$$\delta x = \left[P_1\left(r^2 + 2x^2\right) + 2P_2 x\, y\right]\left[1 + P_3 r^2 + P_4 r^4 + \cdots\right]$$

$$\delta y = \left[2P_1 x\, y + P_2\left(r^2 + 2y^2\right)\right]\left[1 + P_3 r^2 + P_4 r^4 + \cdots\right]$$

where:

$$P_1 = -J_1 \sin \varphi_o$$
$$P_2 = J_1 \cos \varphi_o$$
$$P_3 = \frac{J_2}{J_1}$$
$$P_4 = \frac{J_3}{J_1}$$

P's define the tangential profile function. This is the tangential distortion along the axis of maximum tangential distortion.

The corrected photo coordinates due to the effects of decentering distortion can then be found by subtracting the errors computed in the previous equations. The corrected photo coordinates become:

$$x_c = x - \delta x$$
$$y_c = y - \delta y$$

Atmospheric Refraction

Light rays bend due to refraction. The amount of refractions is a function of the refractive index of the air along the path of that light ray. This index depends upon the temperature, pressure and composition, including humidity, dust, carbon dioxide, etc. The light rays from the object space to image space must pass through layers of differing density thereby bending that ray at various layer boundaries along the path.

From Snell's Law we can express the law of refraction as

$$\left(n_i + dn\right)\sin \theta_i = n_i \sin\left(\theta_i + d\alpha\right)$$

Photogrammetric Tr

Phot

$$\delta x = x\left(\frac{\delta r}{r}\right) = K\left(1 + \frac{r^2}{f^2}\right)x$$

$$\delta y = y\left(\frac{\delta r}{r}\right) = K\left(1 + \frac{r^2}{f^2}\right)y$$

K is a constant determined from some model atmosphere. For example, the 1959 ARDC (Air Rome Development Center) model developed from Bertram is shown as:

$$K = \left[\frac{2410\,H}{H^2 - 6\,H + 250} - \frac{2410\,h}{h^2 - 6\,h + 250}\left(\frac{h}{H}\right)\right]\cdot 10^{-6}$$

The atmospheric model developed by Saastamoinen for an altitude of up to eleven kilometers is given by

$$K = \left\{\frac{1225}{H}\left[\left(1 - 0.022576\,h\right)^{5.256} - \left(1 - 0.02257\,H\right)^{5.256} - 277.0\left(1 - 0.02257\,H\right)^{4.245}\right]\right\}\cdot 10^{-6}$$

For altitudes up to nine kilometers, this equation can be simplified as

$$K = \left\{13\left(H - h\right)\left[1 - 0.02\left(2H + h\right)\right]\right\}\cdot 10^{-6}$$

There are several other atmospheric models. Ghosh [1979] also identifies the US Standard Atmosphere and the ICAO Standard atmosphere. He also states that, up to about 20 km, these models are almost the same. Table 1 shows the amount of distortion using a focal length of 153 mm and the ICAO Standard atmosphere [from Ghosh, 1979, p.95]. The tabulated values, dr, are in micrometers.

Flying Height in m	For Radial Distance r of the Image Point from the Photo Center, in mm									Coefficients	
	12	24	50	63	78	94	111	131	153	$k_1 \cdot 10^{-2}$	$k_2 \cdot 10^{-6}$
	For Ground Elevation – 0 m above sea level										
3000	0.4	0.9	1.9	2.6	3.4	4.5	5.9	7.9	10.7	3.4	1.53
6000	0.7	1.5	3.3	4.4	5.9	7.7	10.1	13.5	18.3	6.1	2.50
9000	0.9	1.9	4.2	5.7	7.5	9.9	13.0	17.3	23.4	7.7	2.23
	For Ground Elevation – 500 m above sea level										
3000	0.3	0.7	1.6	2.1	2.8	3.7	4.9	6.4	8.8	2.8	1.25
6000	0.7	1.3	3.0	4.0	5.3	6.9	9.1	12.2	15.4	5.4	2.3
9000	0.9	1.8	3.9	5.3	7.0	9.2	12.0	16.0	21.7	7.2	2.99
	For Ground Elevation – 1000 m above sea level										
3000	0.3	0.6	1.3	1.7	2.2	2.9	3.9	5.1	6.9	2.2	0.99
6000	0.6	1.2	2.7	3.6	4.8	6.3	8.2	10.9	14.5	4.8	2.08
9000	0.8	1.6	3.6	4.9	6.5	8.5	11.2	14.9	20.1	6.7	2.76
	For Ground Elevation – 1500 m above sea level										
3000	0.2	0.4	0.8	1.2	1.6	2.2	2.8	3.8	5.1	1.6	0.74
6000	0.5	1.1	2.4	3.2	4.2	5.5	7.3	9.7	13.1	4.2	1.87
9000	0.7	1.5	3.4	4.5	6.0	7.8	10.3	13.8	18.6	6.1	2.59

Table 1. Radial image distortion due to atmospheric refraction.

EARTH CURVATURE

Earth curvature causes a displacement of a point due to the curvature of the earth. The point, when projected onto a plane tangent to the ground nadir point, will occupy a position on that plane at a distance of ΔH from the earth's surface. The image displacement, as shown in the figure, is always radially inward towards the principal point. From the geometry, we can see that

$$\theta = \frac{D'}{R} \approx \frac{D}{R}$$

$$\therefore \cos\theta \approx \cos\left(\frac{D}{R}\right) = 1 - \frac{D^2}{2R^2} + \cdots$$

$$\begin{aligned} \Delta H &= R - R\cos\theta \\ &= R\left(1 - \cos\theta\right) \\ &= R\left(1 - 1 + \frac{D^2}{2R^2} - \cdots\right) \end{aligned}$$

$$\therefore \Delta H \approx \frac{D^2}{2R}$$

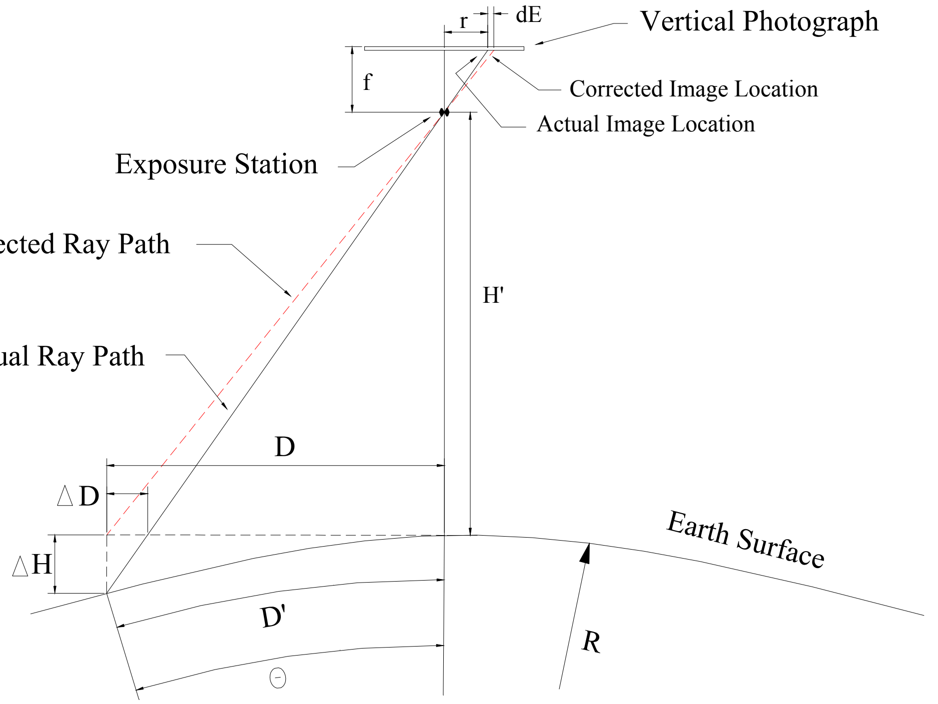

Figure 11. Earth curvature correction.

From which we can write

$$dE = \frac{f}{H'}\Delta D$$

But,

$$dE \approx \frac{D}{H'}\Delta H$$

Therefore,

$$dE = \frac{f}{H'} \frac{D}{H'} \frac{D^2}{2R}$$

$$= \frac{fD^3}{2H^2R}$$

But

$$D \approx \frac{H'}{f} r$$

Yielding

$$dE = \frac{H' r^3}{2 R f^2}$$

Since $H'/(2Rf^2)$ is constant for any photograph

$$dE = K r^3$$

where:

$$K = \frac{H}{2 R f^2}$$

The effects of earth curvature are shown in the Table 2 with respect to the flying height (H) and the radial distance from the nadir point [Ghosh, 1979; Doyle, 1981]. Looking at the formula for earth curvature and the intuitive evaluation of the figure, one can see that the effects will increase rapidly at higher flying heights and the farther one moves from the nadir point.

R(mm)	H in km						
	0.5	1	2	4	6	8	10
10	0.0	0.0	0.0	0.0	0.0	0.0	0.0
20	0.0	0.0	0.1	0.1	0.2	0.2	0.3
40	0.1	0.2	0.4	0.9	1.3	1.8	2.2
60	0.4	0.8	1.5	3.0	4.5	6.0	7.6
80	0.9	1.8	3.6	7.2	10.8	14.3	17.9
100	1.8	3.5	7.0	14.0	21.0	28.0	35.0
120	3.1	6.0	12.1	24.2	36.3	48.4	60.5
140	4.9	9.6	19.2	38.4	57.6	76.8	96.0
160	7.1	14.3	28.6	57.2	85.7	114.3	142.9

Table 2. Amount of earth curvature (in mm) for vertical photography assuming a focal length of 150 mm [from Ghosh, 1979, p.98].

EXAMPLE

A vertical aerial photograph is taken with an aerial camera having the following calibration data:

Calibrated focal length = 152.212 mm

Fiducial mark & principal point coordinates are shown in the next figure of the fiducial marks.

The radial lens distortion is shown from the following diagram delineating the distortion curve.

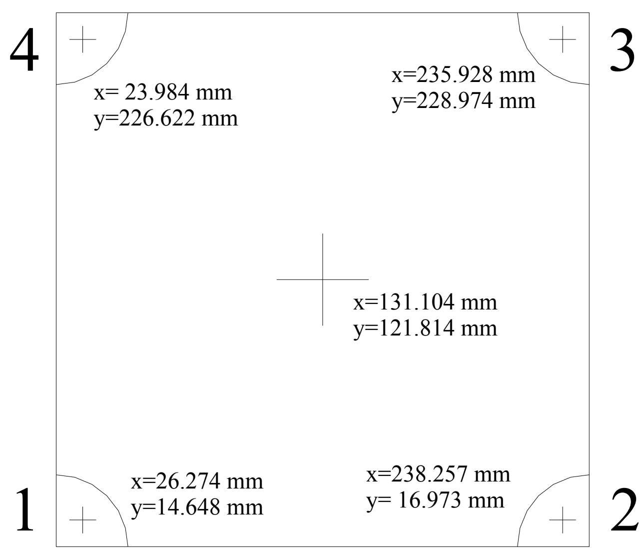

Figure 12. Example showing calibration values for fiducials and principal point.

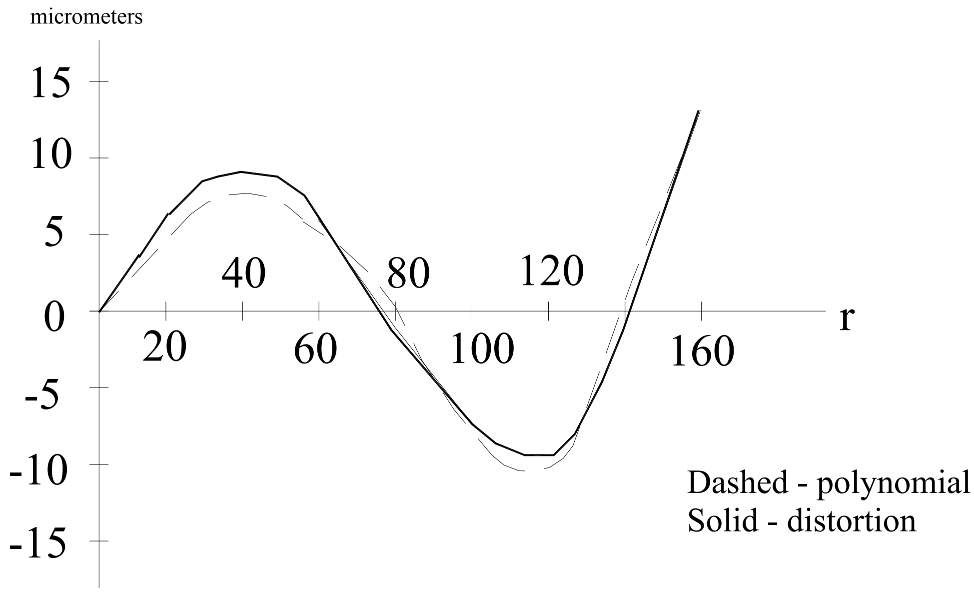

Figure 13. Camera calibration graph of distortion using both polynomials and radial lens distortion.

Radial Distance (mm)	20	40	60	80	100	120	140	160
Distortion (μm)	+6	+9	+6	-1	-7	-9	-1	-13
Polynomial (μm)	+5.3	+7.9	+5.2	+0.5	-7.1	-10.5	+0.6	+123

Table 3. Radial lens distortion for camera in the example.

The decentering lens distortion values are: $J_1 = 8.10x10^{-4}$
$J_2 = -1.40x10^{-8}$
$N_o = 108^o\ 00'$

The flying height is 38,000' above mean sea level. The average height of the terrain is 400' above mean sea level. The photograph is placed in the comparator and the following image coordinates are measured:

point	r_x (mm)	r_y (mm)
1	28.202	13.032
2	240.341	16.260
3	237.068	228.432
4	24.980	225.160

Photogramme

Photogr

$$\Delta r = 0.286\,r - \left(5.794 \times 10^{-5}\right) r^3 + \left(2.223 \times 10^{-9}\right) r^5$$
$$= -8.663 \text{ mm}$$

Siedel radial distortion in terms of their rectangular coordinate vales are:

$$x_c = x\left(1 - \frac{\Delta r}{r}\right) = 95.553\left(1 - \frac{-0.00866}{127.653}\right)$$
$$= 95.559 \text{ mm}$$

$$y_c = y\left(1 - \frac{\Delta r}{r}\right) = \left(-84.646\right)\left(1 - \frac{-0.00866}{127.653}\right)$$
$$= -84.652 \text{ mm}$$

The decentering distortion using the revised Conrady-Brown model is shown as follows:

$$P_1 = -J_1 \sin\varphi_o = -8.10 \times 10^{-4} \sin 108^o = -0.00077$$
$$P_2 = J_1 \cos\varphi_o = 8.10 \times 10^{-4} \cos 108^o = -0.00025$$
$$P_3 = \frac{J_2}{J_1} = \frac{-1.40 \times 10^{-8}}{8.10 \times 10^{-4}} = -0.000017$$

$$\delta x = \left[P_1\left(r^2 + 2x^2\right) + 2P_2 xy\right]\left[1 + P_2 r^2\right]$$
$$= \left[-0.00077\left(127.653^2 + 2\left(95.559\right)^2\right) + 2\left(-0.00025\right)\left(95.559\right)\left(-84.652\right)\right]\left[1 + \left(-0.0025\right)\left(127.653^2\right)\right]$$
$$= -0.016 \text{ mm}$$

$$\delta y = \left[2P_1 xy + P_2\left(r^2 + 2y^2\right)\right]\left[1 + P_3 r^2\right]$$
$$= \left[2\left(-0.00077\right)\left(95.559\right)\left(-84.652\right) + \left(-0.00025\right)\left(127.653^2 + 2\left(-84.655\right)^2\right)\right]\left[1 + \left(-0.000017\right)\left(127.653^2\right)\right]$$
$$= 0.003 \text{ mm}$$

The coordinates corrected for decentering distortion then become:

$$x_c = x - \delta x = 95.559 - (-0.016)$$
$$= 95.576 \text{ mm}$$

$$y_c = y - \delta y = -84.652 - 0.003$$
$$= -84.655 \text{ mm}$$

3. Using the 1959 ARDC model:

$$38{,}000'\left(\frac{1200 \text{ m}}{3937'}\right)\left(\frac{1 \text{ km}}{1000 \text{ m}}\right) = 11.58 \text{ km}$$
$$400'\left(\frac{1200 \text{ m}}{3937'}\right)\left(\frac{1 \text{ km}}{1000 \text{ m}}\right) = 0.12 \text{ km}$$

$$K = \left[\frac{2410\,H}{H^2 - 6H + 250}\right] \times 10^{-6} = \left[\frac{2410(11.58)}{11.58^2 - 6(11.58) + 250}\right] \times 10^{-6}$$
$$= 0.0000887$$

$$\delta x = K\left(1 + \frac{r^2}{f^2}\right)x = 0.0000887\left(1 + \frac{127.653^2}{152.212^2}\right)95.576$$
$$= 0.014 \text{ mm}$$

$$\delta y = K\left(1 + \frac{r^2}{f^2}\right)y = 0.0000887\left(1 + \frac{127.653^2}{152.212^2}\right)(-84.655)$$
$$= -0.013 \text{ mm}$$

The effects of earth curvature are presented as:

$$dE = \frac{r^3 H'}{2f^2 R} = \frac{(127.653)^2\,(38{,}000 - 400)}{2\,(152.212)^2\,(20{,}906{,}000)}$$
$$= 0.0807 \text{ mm}$$

4. The corrected photo coordinated due to the effects of refraction are:

$$x_c = x - \delta x = 95.576 - 0.014$$
$$= 95.561 \text{ mm}$$

$$y_c = y - \delta y = (-84.655) - (-0.013)$$
$$= -84.642 \text{ mm}$$

The coordinates corrected of earth curvature become:

$$x_c = x\left(1 + \frac{dE}{r}\right) = 95.561\left(1 + \frac{0.0807}{127.653}\right)$$
$$= 95.622 \text{ mm}$$

$$y_c = y\left(1 + \frac{dE}{r}\right) = (-84.642)\left(1 + \frac{0.0807}{127.653}\right)$$
$$= -84.696 \text{ mm}$$

The final corrected photo coordinates are, thus,

x = 95.622 mm
y = -84.696 mm

References

Ghosh, S.K., 1979. Analytical Photogrammetry, Pergamon Press, New York, 203p.

Merchant, D.C., 1979. "Instrumentation for Analytical Photogrammetry", Paper presented at the IX Congresso Brasileiro de Cartografia, Brasil, February 4-9, 8p.